

The first World Atlas of the artificial night sky brightness

P. Cinzano,^{1,2★} F. Falchi^{1,2} and C. D. Elvidge³

¹*Dipartimento di Astronomia, Università di Padova, vicolo dell'Osservatorio 5, I-35122 Padova, Italy*

²*Istituto di Scienza e Tecnologia dell'Inquinamento Luminoso (ISTIL), Thiene, Italy*

³*Office of the Director, NOAA National Geophysical Data Center, 325 Broadway, Boulder, CO 80303, USA*

Accepted 2001 July 27. Received 2001 July 24; in original form 2000 December 18

ABSTRACT

We present the first World Atlas of the zenith artificial night sky brightness at sea level. Based on radiance-calibrated high-resolution DMSP satellite data and on accurate modelling of light propagation in the atmosphere, it provides a nearly global picture of how mankind is proceeding to envelop itself in a luminous fog. Comparing the Atlas with the United States Department of Energy (DOE) population density data base, we determined the fraction of population who are living under a sky of given brightness. About two-thirds of the World population and 99 per cent of the population in the United States (excluding Alaska and Hawaii) and European Union live in areas where the night sky is above the threshold set for polluted status. Assuming average eye functionality, about one-fifth of the World population, more than two-thirds of the United States population and more than one half of the European Union population have already lost naked eye visibility of the Milky Way. Finally, about one-tenth of the World population, more than 40 per cent of the United States population and one sixth of the European Union population no longer view the heavens with the eye adapted to night vision, because of the sky brightness.

Key words: scattering – atmospheric effects – light pollution – site testing.

1 INTRODUCTION

One of the most rapidly increasing alterations to the natural environment is the alteration of the ambient light levels in the night environment produced by man-made light. The study of global change must take into account this phenomenon called light pollution. Reported adverse effects of light pollution involve the animal kingdom, the vegetable kingdom and mankind (see e.g. Cinzano 1994 for a reference list). Moreover, the growth of the night sky brightness associated with light pollution produces a loss of perception of the Universe where we live (see e.g. Crawford 1991; Kovalevsky 1992; McNally 1994; Isobe & Hirayama 1998; Cinzano 2000d; Cohen & Sullivan 2001). This could have unintended impacts on the future of our society. In fact the night sky, which constitutes the panorama of the surrounding Universe, has always had a strong influence on human thought and culture, from philosophy to religion, from art to literature and science.

Interest in light pollution has been growing in many fields of science, extending from the traditional field of astronomy to atmospheric physics, environmental sciences, natural sciences and even human sciences. The full extent and implications of the problem have not been addressed to date owing to the fact that there have been no global-scale data on the distribution and magnitude of artificial sky brightness.

The zenith artificial night sky brightness at sea level is a useful indicator of the effects of light pollution on the night sky and the atmospheric content of artificial light. Sea level maps of it, being free of elevation effects, are useful for comparing pollution levels across large territories, for recognizing the most polluted areas or more polluting cities and for identifying dark areas (Cinzano et al. 2000, hereafter Paper I). Even if the capability to perceive the Universe is better shown by specific maps of stellar visibility, which account for altitude and atmospheric extinction (Cinzano et al. 2001a, hereafter Paper II), maps of the zenith artificial sky brightness at sea level provide a reasonable statistical evaluation of the visibility of the Milky Way and a comparison with typical natural brightness levels. The sea level product is also a reasonable starting point in the global study of light pollution given that population numbers are concentrated at low altitudes.

To date no global, quantitative and accurate depiction of the artificial brightness of the night sky has been available to the scientific community and governments. Ground based measurements of sky brightness are available only for a limited number of sites, mainly astronomical observatories, and are spread over many different years. The paucity of ground-based observations makes it impossible to construct global maps from this source.

One approach to modelling the spatial distribution of artificial night sky brightness is to predict it based on population density, because areas with high population usually produce higher levels of light pollution and, consequently, a high artificial luminosity of

★E-mail: cinzano@pd.astro.it; cinzano@lightpollution.it

the night sky (sky glow). However (i) the apparent proportionality between population and sky glow breaks down going from large scales to smaller scales and looking in more detail, owing to the atmospheric propagation of light pollution large distances from the sources, (ii) the upward light emission is not always proportional to the population (e.g. owing to differences in development and lighting practices), (iii) some polluting sources are not represented in population data (e.g. industrial sites and gas flares) and (iv) population census data are not collected using uniform techniques, timetables or administrative reporting units around the World.

As an alternative, we have used a global map of top of atmosphere radiances from man-made light sources produce using data from the US Air Force Defence Meteorological Satellite Program (DMSP) Operational Linescan System (OLS) to model artificial sky brightness. From 1972–92 only film data were available from the DMSP-OLS. Sullivan (1989, 1991) was successful in producing a global map of light sources using film data, but this product did not distinguish between the persistent light sources of cities and the ephemeral lights of events such as fire. In the mid-1990s Elvidge et al. (1997a,b,c) produced a global cloud-free composite of lights using a time-series of DMSP night-time observations, identifying the locations of persistent light sources. This potential use of these ‘stable lights’ for light pollution studies was noted by Isobe & Hamamura (1998). More recently a radiance-calibrated global map of man-made light sources has been produced using DMSP-OLS data collected at reduced gain settings (Elvidge et al. 1999, 2001). With both the location and top of atmosphere radiances mapped, the stage was set to model artificial sky brightness across the surface of the World.

The first exploration of these data for predicting artificial sky brightness was made by applying simple light pollution propagation laws to the satellite data (Falchi 1998; Falchi & Cinzano 2000). Subsequently we introduced a method to map the artificial sky brightness (Paper I) and naked-eye star visibility (Paper II) across large territories, computing the propagation of light inside the atmosphere using the detailed Garstang Models (Garstang 1984, 1986, 1989a,b, 1991, 2000; see also Cinzano

2000a,b). Here we present the first World Atlas of the zenith artificial night sky brightness at sea level. It has been obtained by applying the method discussed in Paper I to global high-resolution radiance-calibrated DMSP satellite data. In Section 2 we summarize the outline of the method, in Section 3 we present the Atlas and a comparison with Earth-based measurements, in Section 4 we present statistical results and tables based on a comparison with the Landsat 2000 DOE population density data base (Dobson et al. 2000) and in Section 5 we draw our conclusions.

2 OUTLINES OF THE METHOD

Here we summarize the methods used to produce the World Atlas. We refer the readers to Paper I and Paper II for a detailed discussion.

High-resolution upward flux data have been calculated from radiances observed by the Operational Linescan System (OLS) carried by the DMSP satellites. The OLS is an oscillating scan radiometer with low-light visible and thermal infrared (TIR) imaging capabilities (Lieske 1981). At night the OLS uses a photomultiplier tube (PMT), attached to a 20-cm reflector telescope, to intensify the visible band signals. It has a broad spectral response from 440 to 940 nm with highest sensitivity in the 500- to 650-nm region, covering the range for primary emissions from the most widely used lamps for external lighting: mercury vapour (545 and 575 nm), high-pressure sodium (from 540 to 630 nm) and low-pressure sodium (589 nm). We used a global map of radiances produced using 28 nights of data collected in 1996–97 at reduced gain levels, to avoid saturation in urban centres. The global map is a ‘cloud-free’ composite, meaning that only cloud-free observations were used. The map reports the average radiance observed from the set of cloud-free observations. Ephemeral lights produced by fires and random noise events were removed by deleting lights that occurred in the same place less than three times. Calibrated upward fluxes per unit solid angle toward the satellite have been obtained from radiance data based on a pre-flight irradiance calibration of the OLS PMT. The calibration was tested

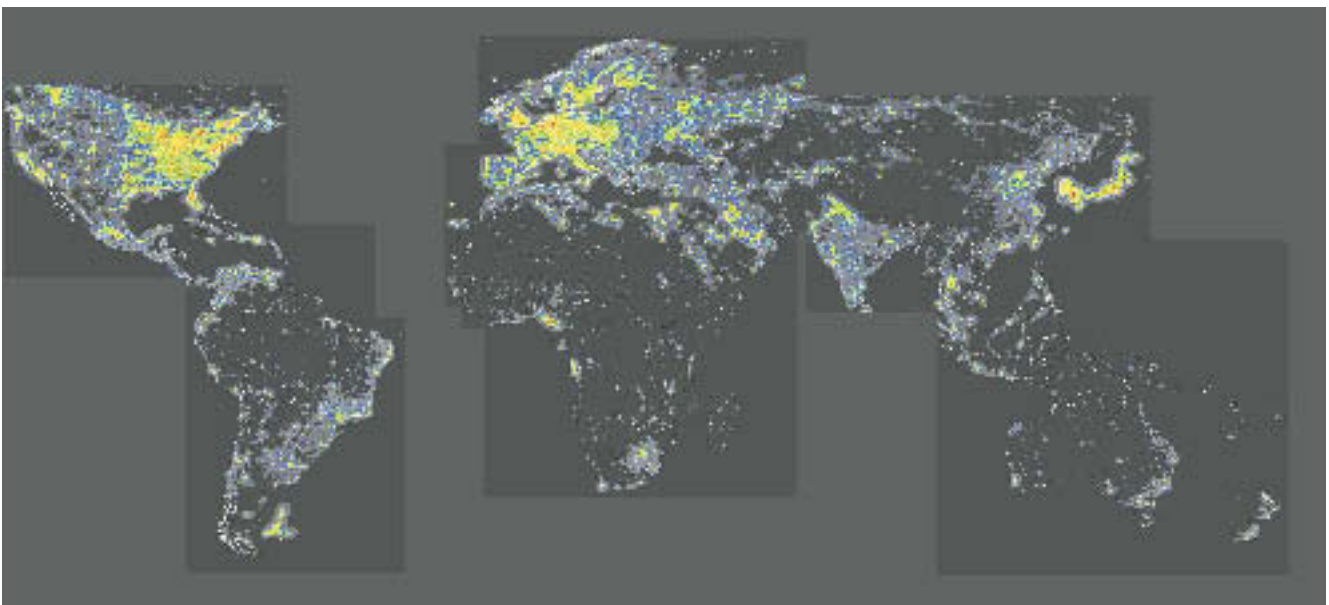


Figure 1. Artificial night sky brightness at sea level in the World. The map has been computed for the photometric astronomical V band, at the zenith, for a clean atmosphere with an aerosol clarity coefficient $K = 1$. The calibration refers to 1996–1997. Country boundaries are approximate.

with Earth-based measurements in Paper I. The upward flux per unit solid angle in other directions was estimated based on an average normalized emission function, in agreement with a study of the upward flux per unit solid angle per inhabitant of a large number of cities at different distances from the satellite nadir.

The propagation of light pollution is computed with the Garstang modelling techniques taking into account Rayleigh scattering by molecules, Mie scattering by aerosols, atmospheric extinction along light paths and Earth curvature. We neglected third and higher order scattering, which can be significant only for optical thicknesses higher than ours. We associated the predictions with well-defined parameters related to the aerosol content, so the atmospheric conditions, which predictions involve, are well known. Atmospheric conditions are variable and a careful evaluation of the ‘typical’ atmospheric condition in the local ‘typical’ clear night of each area is quite difficult, even regarding the difficulty to define it, so we used the same atmospheric model everywhere, corresponding to a standard clean atmosphere (Garstang 1986, 1989; Paper I; Paper II). This also avoids confusion between effects arising from light pollution and effects arising from geographic gradients of atmospheric conditions in ‘typical’ nights. Being more interested in understanding and comparing light pollution distributions than in predicting the effective sky brightness for observational purposes, we computed the artificial sky brightness at sea level, in order to avoid the introduction of altitude effects into our maps. Readers should

consider these differences when interpreting the Atlas results and the related statistics.

3 RESULTS

The World Atlas of the Sea Level Artificial Night Sky Brightness has been computed for the photometric astronomical V band, at the zenith, for a clean atmosphere with an aerosol clarity coefficient $K = 1$, where K is a coefficient which measures the aerosol content of the atmosphere (Garstang 1986), corresponding to a vertical extinction $\Delta m = 0.33$ mag in the V band, a horizontal visibility $\Delta x = 26$ km and an optical depth $\tau = 0.3$. The maps of each continent are shown in Figs 1–9 in latitude/longitude projection. The original high-resolution maps of the World Atlas are downloadable as zipped TIFF files from site <http://www.lightpollution.it/dmsp/> on the World Wide Web. They have been obtained with a mosaic of the original 30×30 arcsec² pixel size maps. Each map level is three times larger than the previous one. The map levels correspond to the artificial sky brightnesses (between brackets the respective colours) in V ph cm⁻² s⁻¹ sr⁻¹: 9.47×10^6 – 2.84×10^7 (blue), 2.84×10^7 – 8.61×10^7 (green), 8.61×10^7 – 2.58×10^8 (yellow), 2.58×10^8 – 7.75×10^8 (orange), 7.75×10^8 – 2.32×10^9 (red), $>2.32 \times 10^9$ (white), or in μ cd m⁻²: 27.7–83.2 (blue), 83.2–252 (green), 252–756 (yellow), 756–2268 (orange), 2268–6804 (red), >6804 (white) (based on the conversion in Garstang 1986, 1989). For the dark grey level see below. The

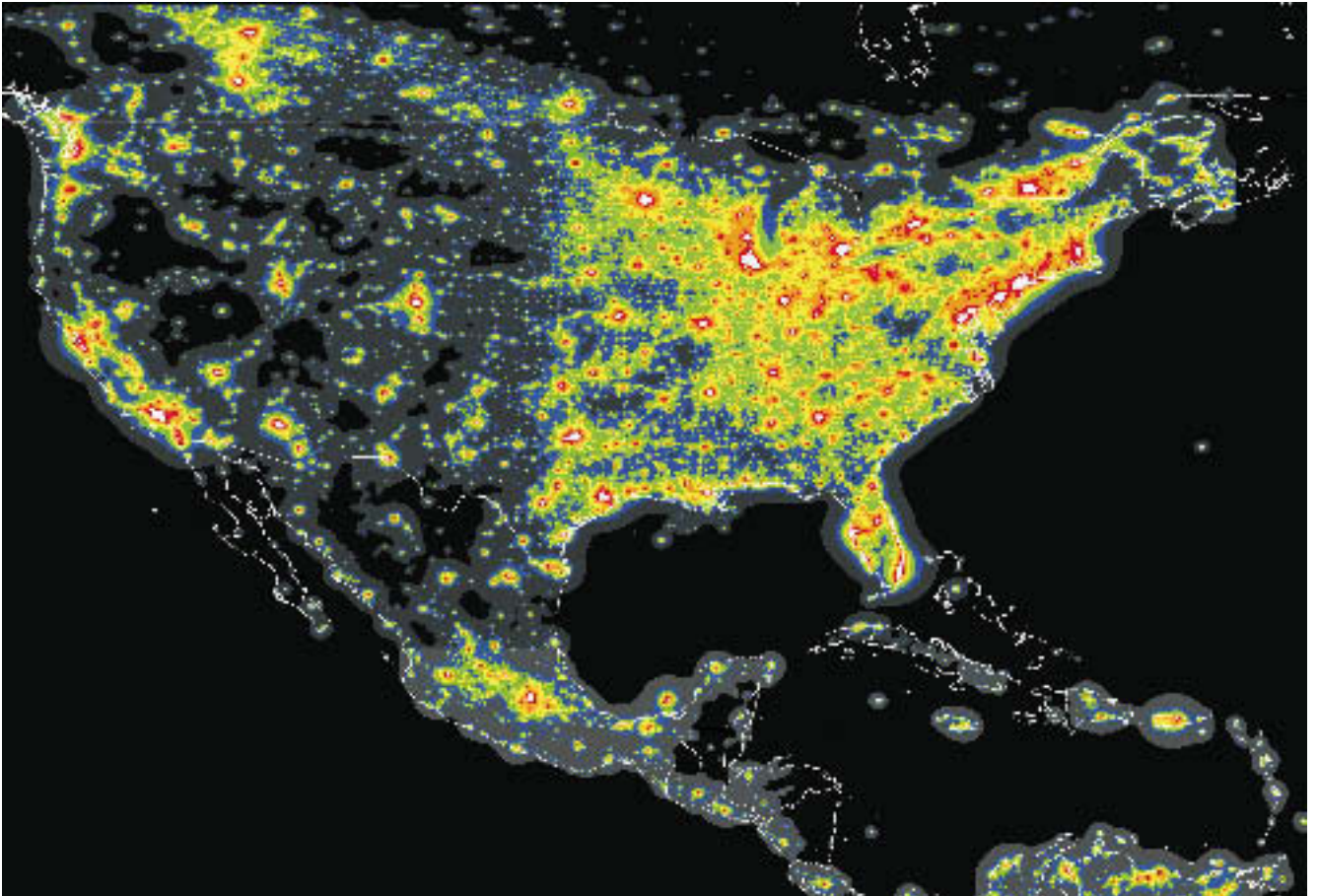


Figure 2. Artificial night sky brightness at sea level for North America. The map has been computed for the photometric astronomical V band, at the zenith, for a clean atmosphere with an aerosol clarity coefficient $K = 1$. The calibration refers to 1996–1997. Country boundaries are approximate.

map levels can be expressed more intuitively as ratios between the artificial sky brightness and the reference natural sky brightness. The natural night sky brightness depends on the geographical position, the solar activity, the time from the sunset and the sky area observed (see e.g. Paper II), so we referred the levels in our maps to an average sky brightness below the atmosphere of $b_n = 8.61 \times 10^7 \text{ V ph cm}^{-2} \text{ s}^{-1} \text{ sr}^{-1}$, corresponding approximately to $21.6 \text{ V mag arcsec}^{-2}$ or $252 \mu\text{cd m}^{-2}$ (Garstang 1986). In this case the map levels became 0.11–0.33 (blue), 0.33–1 (green), 1–3

(yellow), 3–9 (orange), 9–27 (red) and >27 (white). Country boundaries are approximate. In order to show how far the light pollution propagates from sources, we coloured in dark grey areas where the artificial sky brightness is greater than 1 per cent of the reference natural brightness (i.e. greater than $8.61 \times 10^5 \text{ V ph cm}^{-2} \text{ s}^{-1} \text{ sr}^{-1}$ or $2.5 \mu\text{cd m}^{-2}$). In these areas the night sky can be considered unpolluted at the zenith but at lower elevations pollution might not be negligible and uncontrolled growth of light pollution will endanger even the zenith sky. This

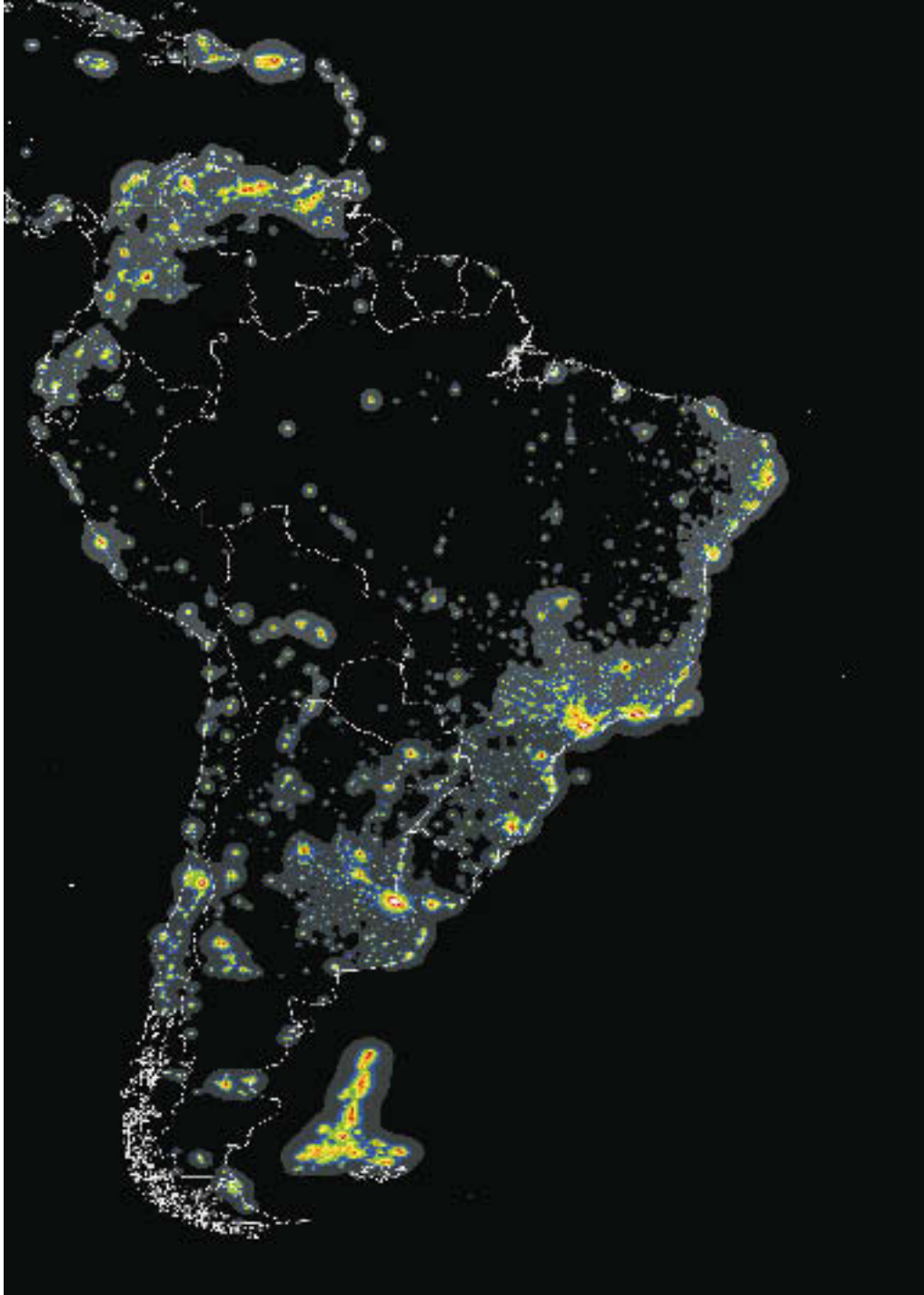


Figure 3. Artificial night sky brightness at sea level for South America. The map has been computed for the photometric astronomical V band, at the zenith, for a clean atmosphere with an aerosol clarity coefficient $K = 1$. The calibration refers to 1996–1997. Country boundaries are approximate.

level must be considered only an indication, because small differences in atmospheric conditions can produce large differences where the gradient of artificial brightness is small.

The resolution of the atlas does not correspond directly to the DMSP-OLS pixel size. The effective instantaneous field of view (EIFOV) of OLS-PMT is larger than the pixel-to-pixel ground sample distance maintained by the along-track OLS sinusoidal scan and the electronic sampling of the signal from the individual scan lines. Moreover the original data have been ‘smoothed’ by on-board averaging of 5 pixel by 5 pixel blocks, yielding a ground sample distance of 2.8 km. During geolocation the OLS pixel values are used to fill 30-arcsec grids, which are composited to generate the global 30-arcsec grid. However, since the sky

brightness is frequently produced by the sum of many contributions from distant sources, the lower resolution of the upward flux data commonly does not play a role and the map resolution mainly corresponds to the 30-arcsec grid cell size, which at the equator is 0.927 km.

The satellite data also record the offshore lights where oil and gas production is active (visible e.g. in the North Sea, Chinese Sea and Arabic Gulf), other natural gas flares (visible e.g. in Nigeria) and the fishing fleets (visible e.g. near the coast of Argentina, in the Japan Sea and near Malacca). Their upward emission functions likely differ from the average emission function of the urban nighttime lighting so that the predictions of their effects have some uncertainty. The presence of snow could also add some uncertainty

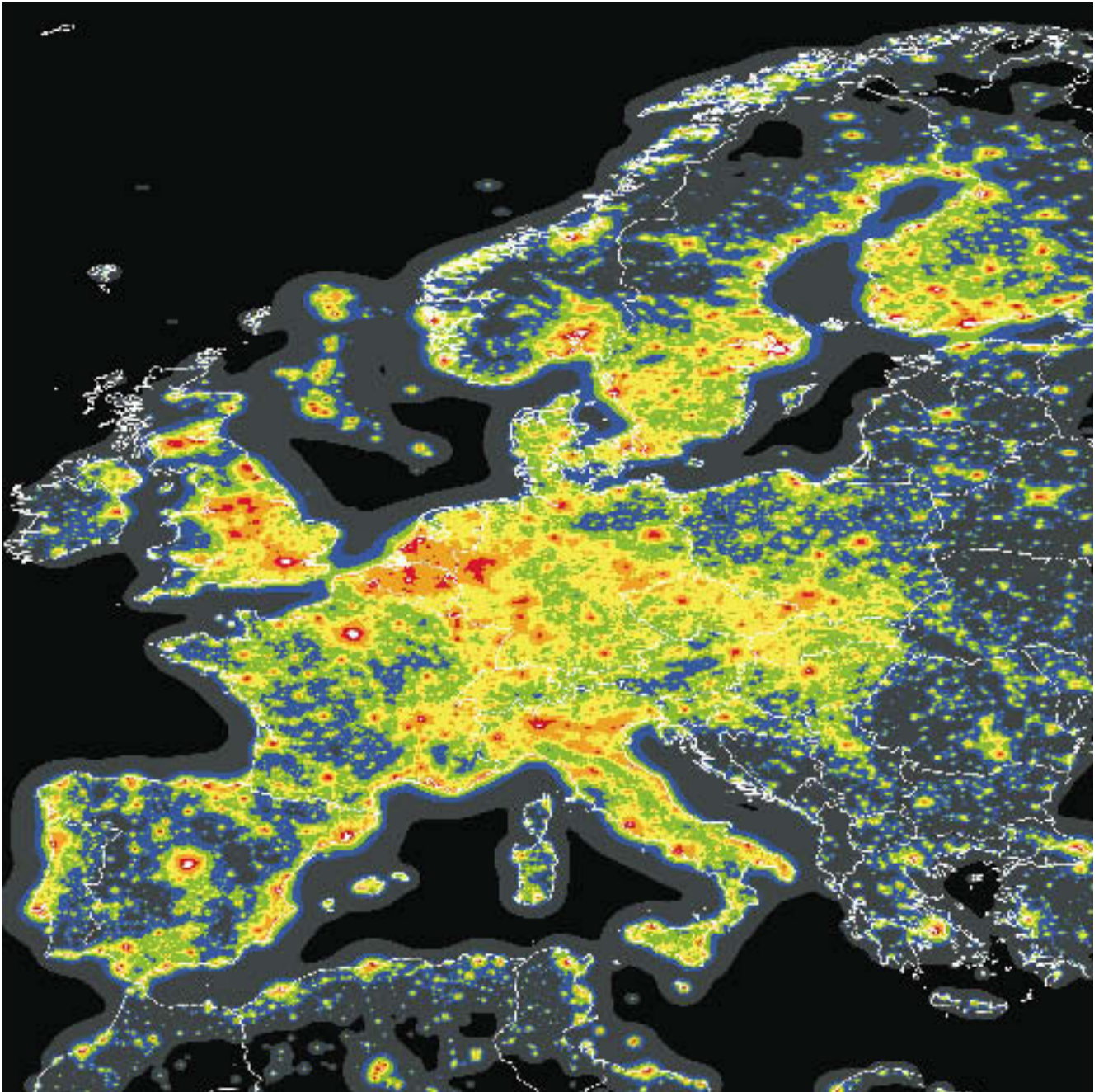


Figure 4. Artificial night sky brightness at sea level for Europe. The map has been computed for the photometric astronomical V band, at the zenith, for a clean atmosphere with an aerosol clarity coefficient $K = 1$. The calibration refers to 1996–1997. Country boundaries are approximate.

(see Paper I). For this reasons we neglected territories near the poles.

The differences between the levels for Europe in Fig. 4, based on the pre-flight OLS-PMT radiance calibration and referring to 1996–1997, and in figs 11 and 12 of Paper I, based on calibration with Earth-based measurements and referring to 1998–1999, agree with the yearly growth of light pollution measured in Europe (see e.g. Cinzano 2000c) but they cannot be considered significant because they are within the uncertainties of the method.

A comparison between map predictions and Earth-based sky brightness measurements is presented in Fig. 10. The left panel shows map predictions versus artificial night sky brightness measurements at the bottom of the atmosphere taken in clean or

photometric nights in the V band for Europe (filled squares), North America (open triangles), South America (open rhombi), Africa (filled triangles) and Asia (filled circle) (Catanzaro & Catalano 2000; Della Prugna 1999; Falchi 1998; Favero et al. 2000; Massey & Foltz 2000; Nawar et al. 1998a; Nawar, Morcos & Mikhail 1998b; Piersimoni, Di Paolantonio & Brocato 2000; Poretti & Scardia 2000; Zitelli 2000). All of them have been taken in 1996–1997, except those for Europe which have been taken in 1998–1999 and rescaled to 1996–1997 by subtracting 20 per cent in order to account approximately for the growth of light pollution in two years. Error bars account for measurement errors and for an uncertainty of about 0.1 mag arcsec^2 in the subtracted natural sky brightness, which is non-negligible in dark sites. These are smaller

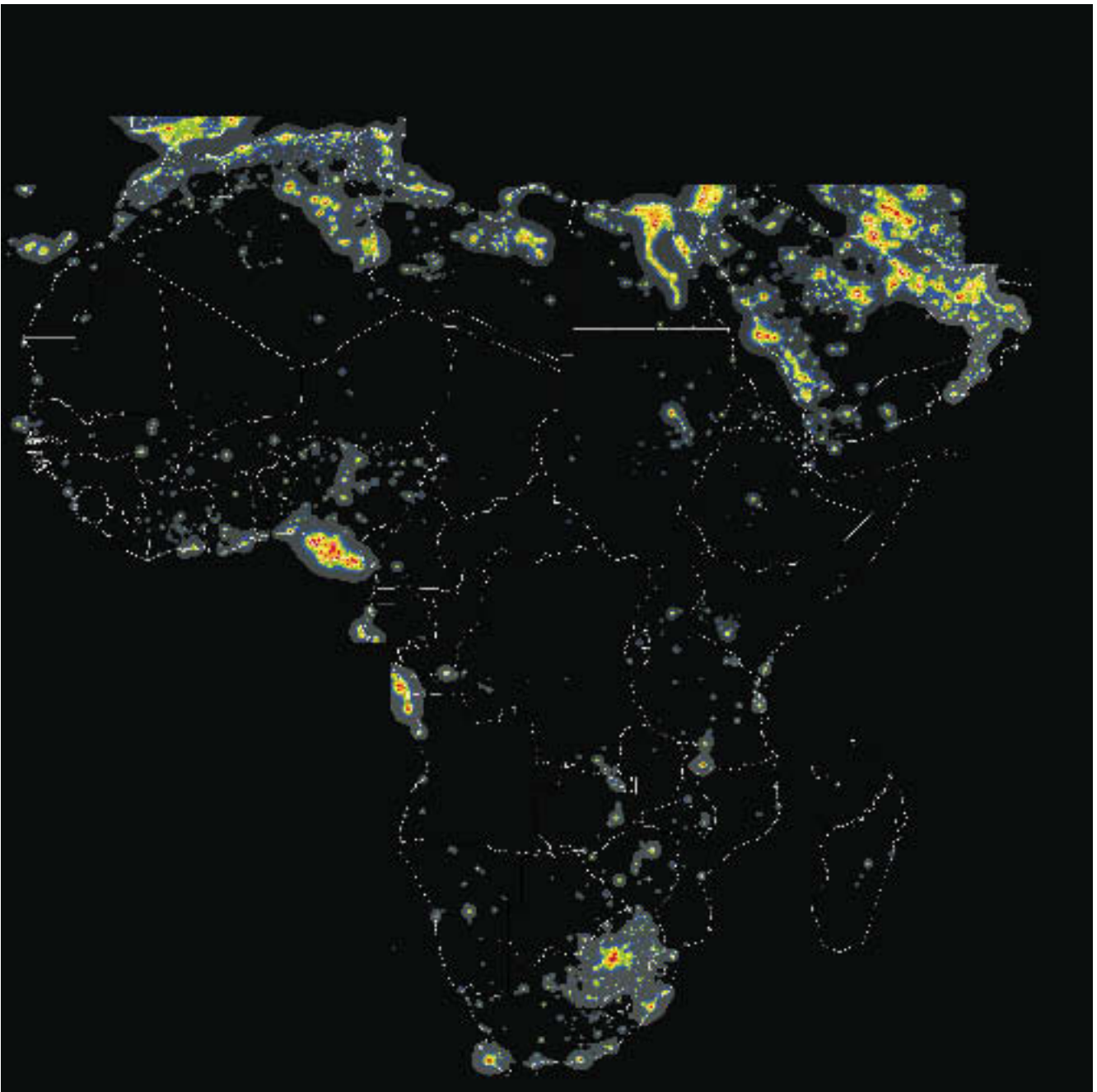


Figure 5. Artificial night sky brightness at sea level for Africa. The map has been computed for the photometric astronomical V band, at the zenith, for a clean atmosphere with an aerosol clarity coefficient $K = 1$. The calibration refers to 1996–1997. Country boundaries are approximate.

than the effects of fluctuations in atmospheric conditions. The right panel shows map predictions versus photographic measurements taken in Japan in the period 1987–1991 with variable atmospheric aerosol content (Kosai, Isobe & Nakayama 1992). They are calibrated to the top of the atmosphere and averaged for each site,

neglecting those where fewer than five measurements were taken. The large error bars show the effects of changes in the atmospheric aerosol content and in the extinction of the light of the comparison star. The dashed line shows the linear regression. A worldwide project of the International Dark-Sky Association (IDA) is

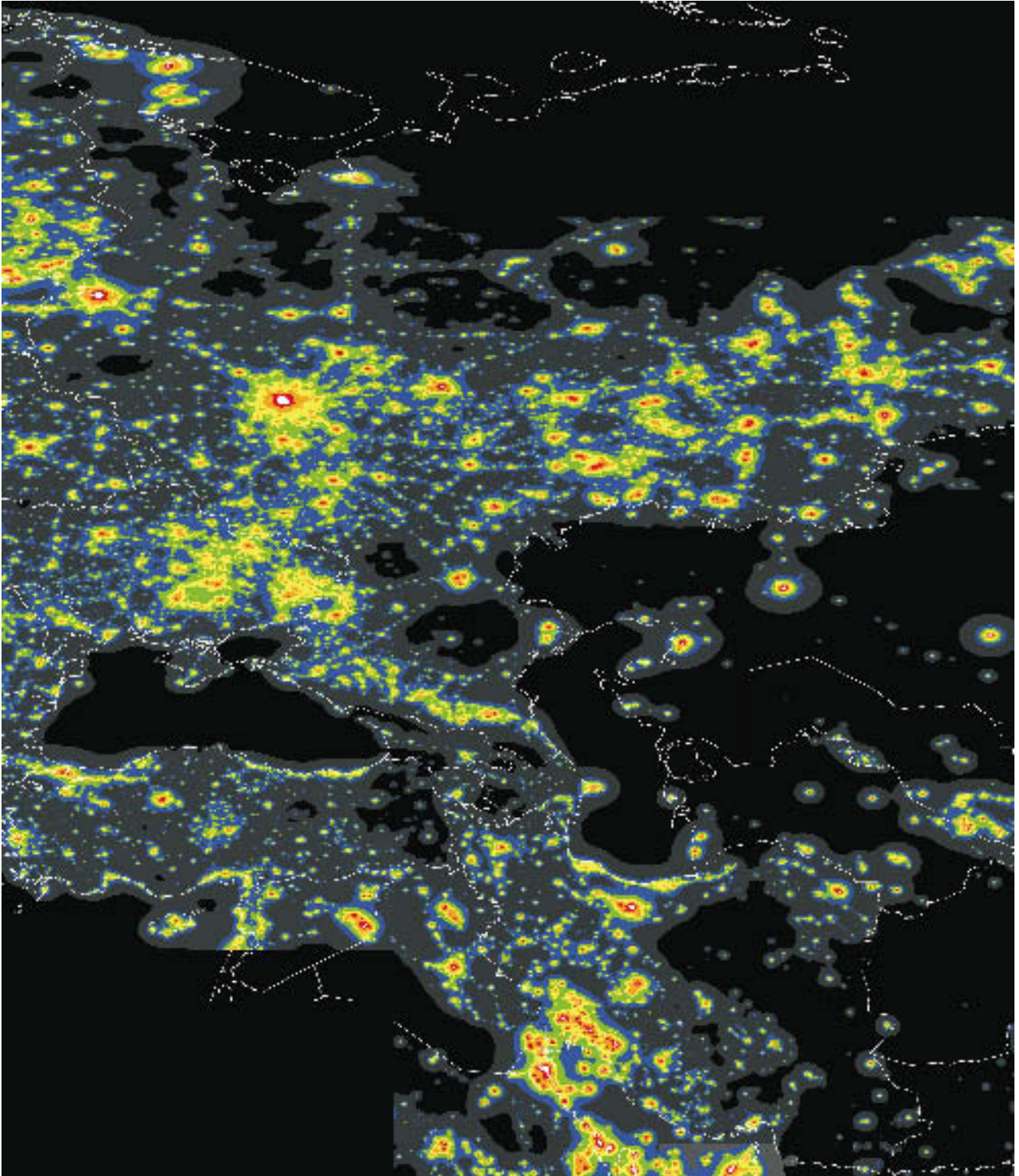


Figure 6. Artificial night sky brightness at sea level for West Asia. The map has been computed for the photometric astronomical V band, at the zenith, for a clean atmosphere with an aerosol clarity coefficient $K = 1$. The calibration refers to 1996–1997. Country boundaries are approximate.

collecting a large number of accurate CCD measurements of sky brightness together with the aerosol content, which could be valuable for testing future improvements in the modelling of artificial sky brightness (Cinzano & Falchi 2000).

4 STATISTICS

We compared our Atlas with the Landsat 2000 DOE global

population density data base (Dobson et al. 2000), which has the same 30-arcsec grid cell size as our Atlas. We checked the spatial match of our Atlas against the Landsat data by visual inspection of the superimposition of the two data sets. We extracted statistics for each individual country, for the European Union and for the World, tallying the percentage population who on standard clear atmosphere nights are living inside each level of our Atlas. Additionally we tallied the percentage population living under a

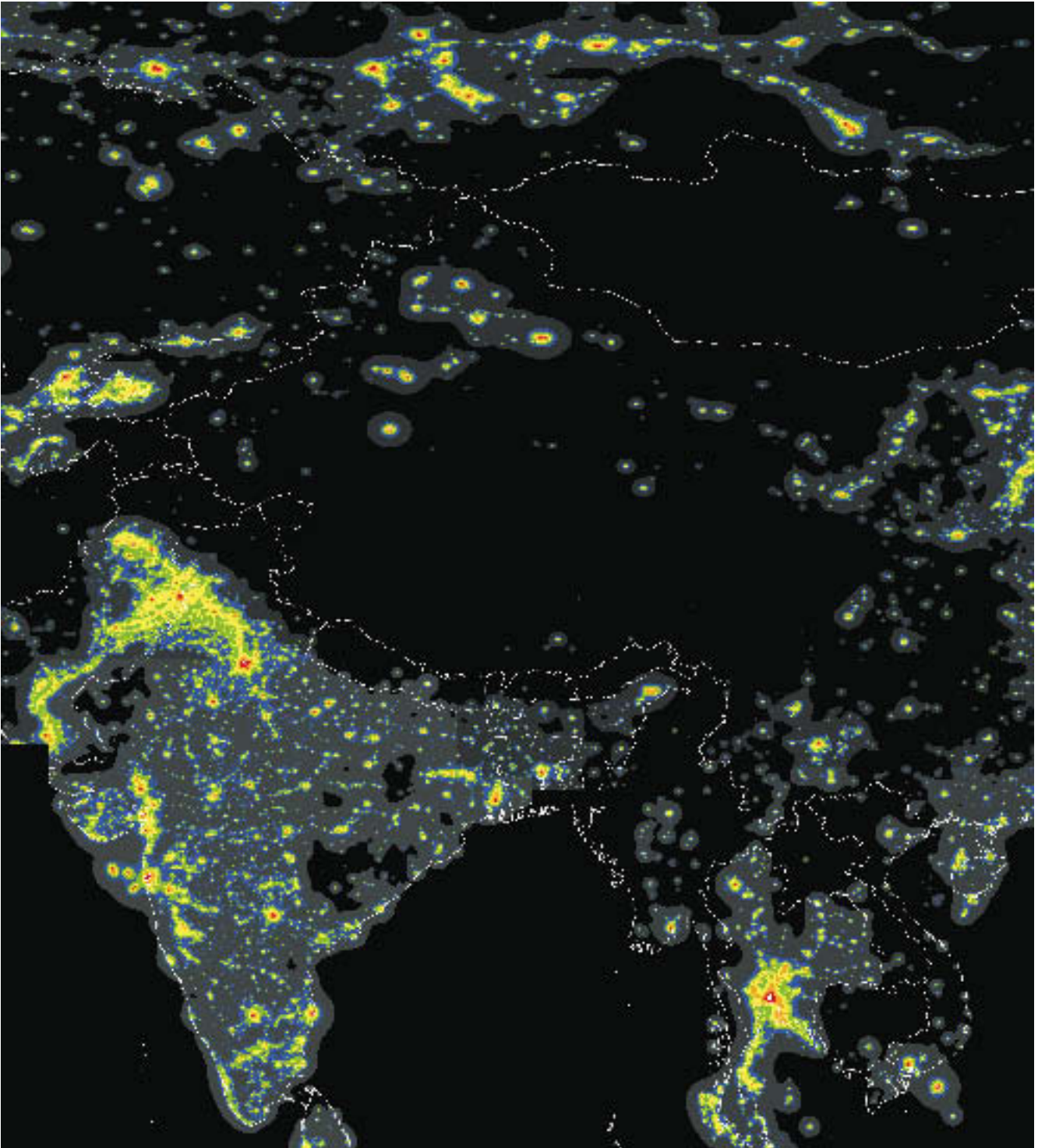


Figure 7. Artificial night sky brightness at sea level for Central Asia. The map has been computed for the photometric astronomical V band, at the zenith, for a clean atmosphere with an aerosol clarity coefficient $K = 1$. The calibration refers to 1996–1997. Country boundaries are approximate.

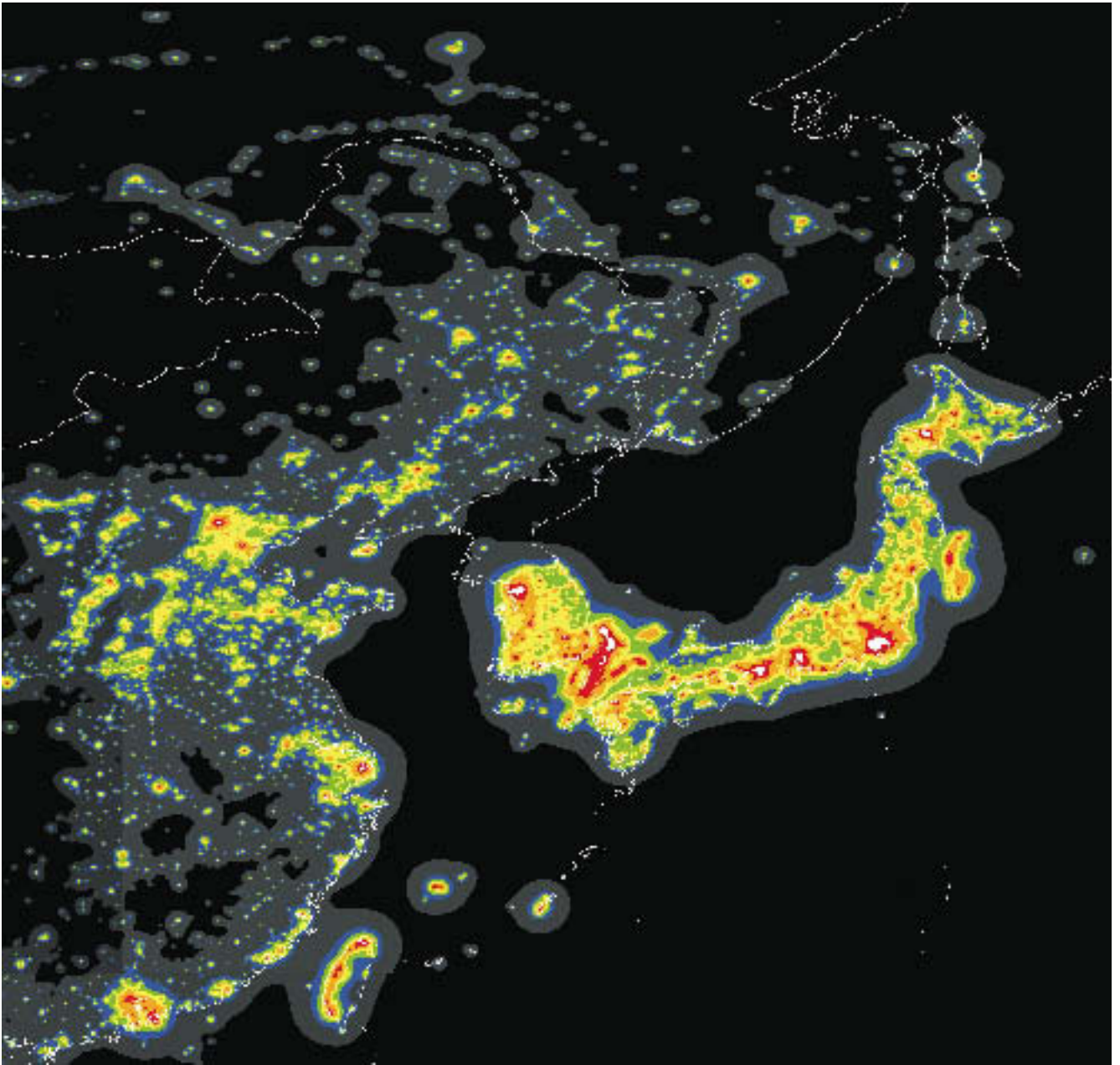


Figure 8. Artificial night sky brightness at sea level for East Asia. The map has been computed for the photometric astronomical V band, at the zenith, for a clean atmosphere with an aerosol clarity coefficient $K = 1$. The calibration refers to 1996–1997. Country boundaries are approximate.

sky brightness greater than several other sky brightness conditions, as described below. Table 1 shows the percentage of population who are living under a sky brightness greater than each level of our Atlas in standard clean nights, i.e. the ratios between the artificial sky brightness and the reference natural sky brightness are greater than 0.11 (column 1), 0.33 (column 2), 1 (column 3), 3 (column 4), 9 (column 5) and 27 (column 6). The table also shows the fraction of population who in standard clean nights are living under a sky brightness greater than some typical sky brightnesses: the threshold b_p to consider the night sky polluted [i.e. when the artificial sky brightness is greater than 10 per cent of the natural night sky brightness above 45° of elevation (Smith 1979)] (column 7), the sky brightness b_{1q} measured with a first quarter moon in the best astronomical sites (e.g. Walker 1987)(column 8), the sky brightness b_m in the considered location with a first quarter

moon at 15° elevation (based on Krisciunas & Schaefer 1991) and zero light pollution (column 9), the sky brightness b_{fm} measured on nights close to full moon in the best astronomical sites (e.g. Walker 1987)(column 10) which is not much larger than the typical zenith brightness at nautical twilight (Schaefer 1993), the threshold of visibility of the Milky Way for average eye capability b_{mw} (column 11), and the eye's night vision threshold b_e (Garstang 1986; see also Schaefer 1993)(column 12). Table 2 summarizes their numerical values.

To produce the Landscan, DOE collected the best available census data for each country and calculated a probability coefficient for the population density of each 30-arcsec grid cell. The probability coefficient is based on slope, proximity to roads, land cover, night-time lights, and an urban density factor (Dobson et al. 2000). The probability coefficients are used to perform a

Table 1. Percentage of population who are living under a sky brightness greater than given levels.

Country	(1) $\geq 0.11b_n$	(2) $\geq 0.33b_n$	(3) $\geq b_n$	(4) $\geq 3b_n$	(5) $\geq 9b_n$	(6) $\geq 27b_n$	(7) $\geq b_p$	(8) $\geq b_{rq}$	(9) $\geq b_m$	(10) $\geq b_{fm}$	(11) $\geq b_{mw}$	(12) $\geq b_e$
Afghanistan	11	8	1	0	0	0	12	8	1	0	0	0
Albania	50	39	27	7	0	0	53	39	27	5	0	0
Algeria	86	74	61	36	12	2	87	73	61	30	16	4
Andorra	100	100	100	90	0	0	100	100	100	85	48	0
Angola	16	15	14	11	7	0	16	14	11	10	0	0
Anguilla UK	100	99	51	0	0	0	100	99	51	0	0	0
Antigua-Barbuda	98	91	70	21	0	0	98	90	70	0	0	0
Argentina	74	71	67	59	44	23	75	70	67	58	52	29
Armenia	91	88	61	42	0	0	92	88	61	35	0	0
Australia	71	69	68	62	37	1	71	69	68	60	48	8
Austria	100	97	82	45	21	0	100	97	82	41	29	9
Azerbaijan	82	76	54	29	1	0	82	75	54	27	19	0
Bahamas	84	82	81	75	58	0	85	82	81	73	66	0
Bahrain	100	100	100	99	99	76	100	100	100	99	99	98
Bangladesh	43	29	18	8	4	0	45	29	18	8	6	0
Barbados	100	98	91	61	0	0	100	98	91	56	27	0
Belgium	100	100	100	96	52	8	100	100	100	94	76	21
Belize	31	17	6	0	0	0	34	16	6	0	0	0
Benin	28	24	17	2	0	0	29	24	17	0	0	0
Bermuda UK	100	100	100	44	0	0	100	100	100	14	0	0
Bhutan	10	7	0	0	0	0	10	6	0	0	0	0
Bolivia	58	57	56	52	37	0	58	57	56	50	45	15
Bosnia-Herzegovina	80	61	32	0	0	0	82	60	32	0	0	0
Botswana	23	20	16	8	0	0	23	20	16	8	1	0
Brazil	66	60	55	45	29	10	66	59	55	43	36	17
British Virgin Islands	70	63	52	0	0	0	70	63	52	0	0	0
Brunei	93	84	78	58	28	0	94	84	78	53	44	0
Bulgaria	84	71	53	22	1	0	86	70	53	19	8	0
Burkina Faso	7	6	5	3	0	0	7	6	5	3	0	0
Burundi	6	4	4	0	0	0	6	4	4	0	0	0
Byelarus	86	78	68	45	13	0	87	78	68	37	18	0
Caiman Islands UK	92	90	78	55	0	0	92	86	78	50	16	0
Cambodia	14	11	9	7	0	0	15	11	9	5	0	0
Cameroon	22	20	18	14	0	0	22	20	18	9	0	0
Canada	97	94	90	83	71	46	97	94	90	82	77	59
Central African Rep.	0	0	0	0	0	0	0	0	0	0	0	0
Chad	7	5	5	0	0	0	7	5	5	0	0	0
Chile	87	83	79	72	49	26	88	82	79	71	61	34
China	54	41	29	13	5	1	55	40	29	12	7	2
Cisgiordania	100	100	100	81	37	0	100	100	100	73	51	24
Colombia	77	68	60	49	34	8	78	67	60	47	40	22
Congo	41	39	36	33	0	0	41	39	36	27	0	0
Costa Rica	80	70	64	56	39	0	81	70	64	55	50	14
Croatia	96	85	67	31	15	0	96	84	67	25	17	0
Cuba	55	47	39	19	2	0	57	47	39	17	11	0
Cyprus	98	91	83	66	36	0	98	91	83	65	56	0
Czech Republic	100	100	95	59	22	0	100	100	95	52	34	5
Denmark	100	97	85	53	23	0	100	97	85	50	33	3
Djibouti	24	22	21	14	0	0	25	22	21	0	0	0
Dominica	7	4	0	0	0	0	7	4	0	0	0	0
Dominican Republic	84	74	64	48	36	0	85	74	64	45	38	16
Ecuador	57	48	41	27	9	0	58	48	41	24	15	2
Egypt	100	100	99	82	33	19	100	100	99	73	43	23
El Salvador	83	71	55	38	26	0	84	70	55	35	29	5
Equatorial Guinea	18	15	15	14	5	0	18	15	15	14	13	1
Eritrea	17	15	13	3	0	0	18	15	13	0	0	0
Estonia	86	72	65	55	35	0	88	72	65	53	42	20
Ethiopia	6	5	4	4	0	0	6	5	4	4	2	0
Falkland Islands UK	8	2	0	0	0	0	9	2	0	0	0	0
Faroe Islands	75	69	58	0	0	0	76	69	58	0	0	0
Fiji Islands	18	14	1	0	0	0	19	14	1	0	0	0
Finland	98	94	88	80	65	24	98	94	88	78	72	44
France	100	95	84	67	41	12	100	95	84	64	51	22
French Guiana	37	37	24	0	0	0	37	37	24	0	0	0
Gabon	39	37	34	31	1	0	39	37	34	22	1	0
Gambia	28	26	23	0	0	0	28	26	23	0	0	0
Gaza	100	100	100	95	0	0	100	100	100	79	36	0
Georgia	81	76	50	14	0	0	81	76	50	10	0	0
Germany	100	100	94	66	25	0	100	100	94	60	40	5
Ghana	29	23	18	12	4	0	30	23	18	11	7	0

Table 1 – continued

Country	(1) $\geq 0.11b_n$	(2) $\geq 0.33b_n$	(3) $\geq b_n$	(4) $\geq 3b_n$	(5) $\geq 9b_n$	(6) $\geq 27b_n$	(7) $\geq b_p$	(8) $\geq b_{fq}$	(9) $\geq b_m$	(10) $\geq b_{fm}$	(11) $\geq b_{mw}$	(12) $\geq b_c$
Gibraltar UK	100	100	100	100	0	0	100	100	100	100	84	0
Greece	90	80	70	54	41	17	91	80	70	52	44	31
Grenada	47	43	14	0	0	0	47	42	14	0	0	0
Guadeloupe	95	95	88	38	1	0	95	95	88	32	17	0
Guatemala	53	39	30	22	17	0	55	38	30	22	20	3
Guernsey UK	100	100	99	14	0	0	100	100	99	0	0	0
Guinea	10	9	7	0	0	0	10	9	7	0	0	0
Guinea-Bissau	21	18	5	0	0	0	21	18	5	0	0	0
Guyana	39	36	32	8	0	0	39	36	32	0	0	0
Haiti	24	22	20	16	0	0	25	22	20	14	0	0
Honduras	49	41	35	27	12	0	50	41	35	27	22	0
Hungary	100	95	76	41	19	5	100	94	76	37	23	12
India	61	41	25	12	4	0	63	40	25	10	6	1
Indonesia	42	33	24	12	4	0	42	33	24	11	6	0
Iran	88	81	73	57	35	14	89	81	73	54	42	21
Iraq	86	77	68	44	24	5	87	77	68	40	28	16
Ireland	86	65	52	37	19	0	88	65	52	34	27	0
Isle of Man UK	100	86	54	0	0	0	100	85	54	0	0	0
Israel	100	100	99	97	79	26	100	100	99	95	90	52
Italy	100	99	95	78	35	6	100	99	95	72	50	15
Ivory Coast	26	22	18	14	1	0	26	21	18	13	10	0
Jamaica	98	87	67	44	26	0	99	85	67	43	33	5
Japan	100	99	96	86	63	27	100	99	96	84	73	41
Jersey UK	100	100	96	0	0	0	100	100	96	0	0	0
Jordan	94	91	88	70	35	8	94	91	88	65	57	23
Kazakhstan	58	54	47	31	3	0	58	54	47	26	9	0
Kenya	19	16	12	7	0	0	19	16	12	6	1	0
Kuwait	100	100	100	99	98	86	100	100	100	99	98	96
Kyrgyzstan	75	66	47	17	0	0	75	66	47	12	6	0
Laos	16	14	11	2	0	0	16	14	11	0	0	0
Latvia	77	68	61	47	33	0	78	68	61	44	37	11
Lebanon	100	97	81	43	2	0	100	96	81	37	14	0
Lesotho	17	11	9	0	0	0	17	11	9	0	0	0
Liberia	0	0	0	0	0	0	0	0	0	0	0	0
Libya	83	78	73	62	39	8	84	78	73	58	48	21
Liechtenstein	100	100	100	0	0	0	100	100	100	0	0	0
Lithuania	86	71	61	42	12	0	89	71	61	38	23	0
Luxembourg	100	100	100	94	63	0	100	100	100	90	81	11
Macau P	100	100	100	100	100	0	100	100	100	100	100	0
Macedonia	92	82	71	32	0	0	94	81	71	29	12	0
Madagascar	11	10	8	0	0	0	11	10	8	0	0	0
Malawi	15	13	10	0	0	0	15	13	10	0	0	0
Malaysia	78	68	58	40	20	1	78	68	58	36	25	8
Mali	15	13	9	6	0	0	15	13	9	5	0	0
Malta	100	100	100	91	48	0	100	100	100	88	77	0
Martinique F	100	99	93	61	0	0	100	99	93	58	39	0
Mauritania	23	22	21	17	0	0	23	22	21	17	0	0
Mayotte F	6	5	0	0	0	0	7	3	0	0	0	0
Mexico	88	81	72	59	44	25	89	80	72	57	50	33
Moldova	93	83	62	33	0	0	95	83	62	27	9	0
Monaco	100	100	100	100	87	0	100	100	100	100	100	0
Mongolia	34	33	31	16	0	0	34	33	31	11	0	0
Montenegro	83	74	58	9	0	0	84	74	58	0	0	0
Montserrat UK	56	25	0	0	0	0	59	25	0	0	0	0
Morocco	62	53	45	35	16	4	63	52	45	32	25	7
Mozambique	10	9	7	4	0	0	10	9	7	3	1	0
Myanmar	25	19	12	8	2	0	25	19	12	7	5	0
Namibia	17	16	13	8	3	0	17	16	13	8	6	0
Nepal	25	19	9	3	0	0	26	18	9	2	0	0
Netherlands	100	100	100	88	39	2	100	100	100	85	60	16
Netherlands Antilles	100	98	93	89	56	0	100	98	93	84	69	0
New Caledonia	45	44	44	42	0	0	45	44	44	41	0	0
New Zealand	87	84	81	67	25	0	87	84	81	61	45	2
Nicaragua	56	48	42	22	11	0	57	48	42	22	20	0
Niger	3	2	1	1	0	0	3	2	1	1	0	0
Nigeria	45	37	27	17	7	1	46	36	27	15	12	2
Norfolk Islands AU	7	0	0	0	0	0	10	0	0	0	0	0
North Korea	25	18	13	1	0	0	26	17	13	0	0	0
Norway	95	89	82	72	52	20	96	89	82	70	61	30
Oman	90	83	73	39	24	0	90	82	73	35	27	12

Downloaded from https://academic.oup.com/mnras/article/328/3/689/1240556 by guest on 20 August 2022

Table 1 – *continued*

Country	(1) $\geq 0.11b_n$	(2) $\geq 0.33b_n$	(3) $\geq b_n$	(4) $\geq 3b_n$	(5) $\geq 9b_n$	(6) $\geq 27b_n$	(7) $\geq b_p$	(8) $\geq b_{rq}$	(9) $\geq b_m$	(10) $\geq b_{im}$	(11) $\geq b_{mw}$	(12) $\geq b_c$
Pakistan	87	77	54	26	14	4	88	76	54	24	18	8
Panama	65	57	49	38	23	0	65	57	49	36	29	0
Papua New Guinea	13	12	10	3	0	0	13	12	10	2	0	0
Paraguay	60	55	50	41	31	0	61	55	50	38	36	16
Peru	58	56	52	44	30	15	59	56	52	41	33	23
Philippines	50	42	34	23	14	2	50	42	34	22	17	8
Poland	99	88	72	44	18	0	100	87	72	39	26	3
Portugal	98	90	80	60	33	14	99	89	80	57	42	22
Puerto Rico	100	100	100	93	46	23	100	100	100	90	67	33
Qatar	100	100	99	97	92	81	100	100	99	96	94	84
Romania	84	69	52	23	7	0	86	69	52	19	13	0
Russia	87	80	73	60	34	8	88	79	73	57	44	15
Rwanda	6	4	4	0	0	0	6	4	4	0	0	0
Saint Kitts e Nevis	97	84	65	0	0	0	99	81	65	0	0	0
Saint Lucia	88	84	69	0	0	0	89	84	69	0	0	0
San Marino	100	100	100	99	0	0	100	100	100	90	0	0
Saudi Arabia	94	92	90	84	74	53	94	92	90	83	78	64
Senegal	35	32	26	18	0	0	35	31	26	18	2	0
Serbia	95	83	63	22	5	0	96	82	63	19	12	0
Seychelles	0	0	0	0	0	0	0	0	0	0	0	0
Sierra Leone	15	15	14	0	0	0	15	15	14	0	0	0
Singapore	100	100	100	100	100	60	100	100	100	100	100	95
Slovakia	100	100	92	35	7	0	100	100	92	29	14	0
Slovenia	100	98	81	47	19	0	100	97	81	43	30	0
Somalia	11	9	0	0	0	0	11	9	0	0	0	0
South Africa	58	51	46	38	23	1	58	51	46	36	29	10
South Korea	100	100	99	92	75	45	100	100	99	90	82	59
Spain	98	93	87	78	57	25	99	93	87	76	67	38
Sri Lanka	44	26	12	0	0	0	46	24	12	0	0	0
St. Vinc.- Grenadines	77	62	21	0	0	0	78	62	21	0	0	0
Sudan	23	21	18	13	8	0	23	20	18	13	10	0
Suriname	66	59	53	30	0	0	66	59	53	18	0	0
Swaziland	22	14	10	0	0	0	23	14	10	0	0	0
Sweden	99	97	93	79	51	18	99	97	93	75	62	31
Switzerland	100	100	97	67	15	0	100	100	97	57	28	0
Syria	89	79	65	42	13	0	89	78	65	39	23	0
Taiwan	100	99	99	92	60	16	100	99	99	87	72	34
Tajikistan	73	61	41	8	0	0	74	60	41	3	0	0
Tanzania	14	12	11	6	0	0	14	12	11	6	5	0
Thailand	68	56	45	25	14	8	69	56	45	22	17	11
Togo	19	17	15	2	0	0	19	17	15	0	0	0
Trinidad and Tobago	99	96	90	67	2	0	99	96	90	59	29	0
Tunisia	80	70	60	38	11	0	82	69	60	33	22	2
Turkey	79	71	62	40	15	0	80	70	62	36	25	2
Turkmenistan	56	50	38	19	4	0	57	49	38	16	11	0
Turks - Caicos Is. UK	54	52	0	0	0	0	54	52	0	0	0	0
Uganda	10	8	5	4	0	0	10	8	5	4	1	0
Ukraine	93	85	70	40	7	0	93	85	70	34	18	0
United Arab Emirates	100	100	99	97	89	67	100	100	99	97	94	78
United Kingdom	100	98	94	79	40	4	100	98	94	74	55	15
Un. States of America	99	97	93	83	62	30	99	97	93	81	71	44
Uruguay	80	75	73	62	50	18	80	75	73	61	54	37
Uzbekistan	90	84	68	28	10	0	90	83	68	24	12	1
Vanuatu	8	6	4	4	0	0	8	5	4	4	2	0
Venezuela	90	85	80	71	52	23	91	84	80	70	62	31
Vietnam	31	22	14	9	4	0	32	22	14	8	5	2
Virgin islands US	100	100	99	94	0	0	100	100	99	84	39	0
Western Sahara	11	9	8	2	0	0	12	9	8	2	0	0
Yemen	41	34	23	13	3	0	42	33	23	12	7	0
Zaire	13	12	11	7	0	0	13	12	11	7	1	0
Zambia	38	36	32	12	0	0	38	36	32	11	4	0
Zimbabwe	30	28	25	17	0	0	30	28	25	14	1	0
European Union	99	97	90	72	38	8	99	96	90	68	51	17
The World	62	53	43	30	16	6	63	52	43	28	21	9

spatial allocation of the population for all the grid cells covering a census reporting unit (usually province). Therefore the resulting population distribution represents an ambient population which integrates diurnal movements and collective travel habits rather

than the residential population at night-time. Readers must be aware that these percentages should be considered as estimates, owing to the proceeding discussion on the Landsat data characteristics, the minor altitude effects on the artificial sky

Table 2. Numerical values and references of thresholds in Table 1, columns 8–14. The natural sky brightness has been subtracted.

b_p	b_{iq}	b_m	b_{fm}	b_{mw}	b_e
10 per cent b_n	$\sim 90 \mu\text{cd m}^{-2}$	$252 \mu\text{cd m}^2$	$\sim 890 \mu\text{cd m}^2$	$6 b_n$	$4452 \mu\text{cd m}^2$
Smith 1979	e.g. Walker 1987	based on Krisciunas & Schaefer 1991	e.g. Walker 1987	estimate	Garstang 1986

brightness levels and departures in the angular distribution of light from sources from the assumed average normalized emission function.

We also determined the surface area corresponding to each level of our Atlas. Table 3 shows the fraction per cent of the surface area of the individual World countries, the European Union and the World, where the sky brightness is greater than each level of our Atlas in standard clean nights, i.e. the ratios between the artificial sky brightness and the reference natural sky brightness are greater than 0.11 (column 1), 0.33 (column 2), 1 (column 3), 3 (column 4), 9 (column 5) and 27 (column 6).

Fig. 11 shows in white the World’s area covered by our Atlas where 98 per cent of the World population lives. Our data refer to 1996–1997, so the artificial night sky brightness today is likely increased.

5 CONCLUSIONS

The Atlas reveals that light pollution of the night sky is not confined, as commonly believed, to developed countries, but rather appears to be a global-scale problem affecting nearly every country of the World. The problem is more severe in the United States, Europe and Japan, as expected. However the night sky appears more seriously endangered than commonly believed.

The population percentages presented in Tables 1 and 3 speak for themselves, indicating that large numbers of people in many countries have had their vision of the night sky severely degraded. Our Atlas refers to 1996–1997, so the situation today is undoubtedly worse. We found that more than 99 per cent of the United States and European Union population, and about two-thirds of the World population, live in areas where the night sky is above the threshold for polluted status [i.e. the artificial sky brightness is greater than 10 per cent of the natural night sky brightness above 45° of elevation (Smith 1979)]. In the areas where 97 per cent of the United States population, 96 per cent of the European Union population and half of the World population live, the night sky in standard clean atmospheric conditions is brighter than has been measured with a first quarter moon in the best astronomical sites (e.g. Walker 1987). 93 per cent of the United States population, 90 per cent of the European Union population and about 40 per cent of the World population live under a zenith night sky that is brighter than they would have in the same location with a first quarter moon at 15° elevation (based on Krisciunas & Schaefer 1991) and zero light pollution. They therefore effectively live in perennial moonlight. They rarely realize it because they still experience the sky to be brighter under a full moon than under new moon conditions. We also found that for about 80 per cent of the United States population, two-thirds of the European Union population and more than one-fourth of the World population the sky brightness is even greater than that measured on nights close to full moon in the best astronomical sites (e.g. Walker 1987). ‘Night’ never really comes for them because this sky brightness is slightly larger than the typical zenith brightness at nautical twilight (Schaefer 1993). Assuming average eye functionality, more than

two-thirds of the United States population, about half of the European Union population and one-fifth of the World population have already lost the possibility of seeing the Milky Way, the Galaxy where we live. Finally, approximately 40 per cent of the United States population, one-sixth of the European Union population and one tenth of the World population cannot even look at the heavens with the eye adapted to night vision, because its brightness is above the night vision threshold (Garstang 1986; see also Schaefer 1993). Preliminary data on moonlight without the moon were presented by Cinzano, Falchi & Elvidge (2001b).

We noticed that Venice is the only city in Italy with more than 250 000 inhabitants from which an average observer had the possibility of viewing the Milky Way from the city centre on a clear night in 1996–97. Even though Venice’s historic centre (population 68 000) is imbedded in the strong sky glow produced by the terra firma part of the city (Mestre, population 189 000), its average artificial sky brightness is still lower than in cities with 80 000 inhabitants in the nearby Veneto plane. This is due mainly to the unique low-intensity romantic lighting of this city, which deserves to be preserved.

Many areas that were believed to be unpolluted because they appear completely dark in night-time satellite images, on the contrary show in the Atlas non-negligible artificial brightness levels, owing to the outward propagation of light pollution. In a number of cases the sky of a country appears polluted by sources in a neighbouring country: this could open a new chapter of international jurisprudence. Astronomical observatories known for their negligible zenith artificial sky brightness appear to lie near or inside the 1 per cent level: this means that without undertaking a serious control of light pollution in liable areas they risk in less than 20 years seeing their sky quality degraded. Site testing for next-generation telescopes will require an accurate study of the long-term growth of the artificial night sky brightness in order to assure dark sky conditions for an adequate number of years after their installation. Serious control both of lighting installations and of new urbanizations or developments would be necessary for a large area surrounding the site (possibly even 250 km in radius).

We are working towards the preparation of a forthcoming Atlas giving the growth rates of light pollution, the growth rates of night sky brightness, the emission functions of the sources (Paper I) and the ratio of the upward light flux versus population per unit area.

The International Dark-Sky Association (<http://www.darksky.org>) is supporting worldwide the legislative effort carried on in many countries to limit light pollution, in order to protect astronomical observatories, amateur observatories, the citizens’ perception of the Universe and the environment, and to save energy, money and resources. Commission 50 of the International Astronomical Union (‘The protection of existing and potential astronomical sites’) is working actively to preserve the astronomical sky, now with a specific Working Group (‘Controlling light pollution’) born after the UN–IAU Special Environmental Symposium ‘Preserving the Astronomical Sky’, held in the

Table 3. Percentage of the surface area where the artificial sky brightness at sea level on standard clear nights is greater than given levels.

Country	(1) $\geq 0.11b_n$	(2) $\geq 0.33b_n$	(3) $\geq b_n$	(4) $\geq 3b_n$	(5) $\geq 9b_n$	(6) $\geq 27b_n$
Afghanistan	0.4	0.1	0.0	0.0	0.0	0.0
Albania	17.1	5.2	1.3	0.1	0.0	0.0
Algeria	9.4	4.4	1.8	0.7	0.2	0.0
Andorra	100.0	100.0	89.8	27.9	0.0	0.0
Angola	0.9	0.4	0.2	0.0	0.0	0.0
Anguilla UK	100.0	83.6	19.0	0.0	0.0	0.0
Antigua-Barbuda	63.5	49.8	21.6	1.3	0.0	0.0
Argentina	11.3	4.6	1.9	0.7	0.2	0.0
Armenia	17.8	7.2	2.1	0.5	0.0	0.0
Australia	2.3	1.0	0.4	0.2	0.0	0.0
Austria	100.0	76.2	29.3	3.5	0.4	0.0
Azerbaijan	23.3	9.3	3.2	0.8	0.0	0.0
Bahamas	7.8	4.9	3.4	1.7	0.3	0.0
Bahrain	100.0	100.0	91.6	74.6	50.7	25.8
Bangladesh	24.4	9.0	3.0	0.6	0.1	0.0
Barbados	100.0	93.3	64.6	20.0	0.0	0.0
Belgium	100.0	100.0	99.8	74.4	11.4	0.3
Belize	7.6	2.5	0.6	0.0	0.0	0.0
Benin	1.6	0.6	0.2	0.0	0.0	0.0
Bermuda UK	100.0	100.0	92.5	17.0	0.0	0.0
Bhutan	0.4	0.1	0.0	0.0	0.0	0.0
Bolivia	3.0	1.4	0.6	0.2	0.0	0.0
Bosnia-Herzegovina	40.5	12.6	2.2	0.0	0.0	0.0
Botswana	0.6	0.2	0.1	0.0	0.0	0.0
Brazil	7.9	3.5	1.4	0.5	0.1	0.0
British Virgin Islands	51.0	44.5	32.8	0.0	0.0	0.0
Brunei	47.6	27.2	15.8	8.4	1.1	0.0
Bulgaria	41.1	12.0	3.4	0.4	0.0	0.0
Burkina Faso	0.9	0.4	0.1	0.0	0.0	0.0
Burundi	1.6	0.6	0.2	0.0	0.0	0.0
Byelarus	41.0	14.8	4.9	0.8	0.1	0.0
Caiman Islands UK	68.8	59.3	27.5	10.9	0.0	0.0
Cambodia	1.3	0.5	0.2	0.0	0.0	0.0
Cameroon	1.4	0.5	0.1	0.0	0.0	0.0
Canada	32.8	18.6	9.2	3.6	1.0	0.2
Central African Rep.0	0.0	0.0	0.0	0.0	0.0	0.0
Chad	0.1	0.0	0.0	0.0	0.0	0.0
Chile	12.2	5.6	2.1	0.7	0.2	0.0
China	12.5	6.0	2.4	0.5	0.1	0.0
Cisgiordania	100.0	100.0	92.7	43.2	4.1	0.0
Colombia	14.0	5.9	2.3	0.7	0.1	0.0
Congo	1.2	0.5	0.2	0.0	0.0	0.0
Costa Rica	34.1	15.1	6.0	2.1	0.5	0.0
Croatia	74.8	41.4	14.3	1.7	0.2	0.0
Cuba	14.6	5.8	2.1	0.5	0.1	0.0
Cyprus	85.1	57.3	29.5	7.1	0.7	0.0
Czech Republic	100.0	99.7	76.0	11.8	0.9	0.0
Denmark	99.5	87.4	46.0	9.1	0.9	0.0
Djibouti	1.6	0.6	0.2	0.0	0.0	0.0
Dominica	8.1	2.5	0.0	0.0	0.0	0.0
Dominican Republic	45.0	22.6	8.4	2.4	0.6	0.0
Ecuador	17.4	8.2	3.3	0.7	0.1	0.0
Egypt	17.1	10.7	6.4	2.5	0.3	0.1
El Salvador	59.1	33.4	12.4	3.4	0.8	0.0
Equatorial Guinea	5.5	3.0	1.3	0.5	0.1	0.0
Eritrea	0.8	0.3	0.1	0.0	0.0	0.0
Estonia	59.7	23.8	9.3	2.4	0.5	0.0
Ethiopia	0.4	0.2	0.1	0.0	0.0	0.0
Falkland Islands UK	5.1	0.0	0.0	0.0	0.0	0.0
Faroe Islands	33.8	13.5	2.3	0.0	0.0	0.0
Fiji Islands	3.0	1.0	0.1	0.0	0.0	0.0
Finland	70.0	47.2	22.7	6.7	1.3	0.2
France	98.9	75.1	36.0	9.6	1.4	0.1
French Guiana	0.6	0.3	0.1	0.0	0.0	0.0
Gabon	3.3	1.5	0.8	0.3	0.0	0.0
Gambia	2.5	1.2	0.6	0.0	0.0	0.0
Gaza	100.0	100.0	100.0	74.5	0.0	0.0
Georgia	10.6	4.5	1.2	0.1	0.0	0.0
Germany	100.0	94.5	64.5	16.9	1.9	0.0

Table 3 – continued

Country	(1) $\geq 0.11b_n$	(2) $\geq 0.33b_n$	(3) $\geq b_n$	(4) $\geq 3b_n$	(5) $\geq 9b_n$	(6) $\geq 27b_n$
Ghana	4.3	1.7	0.7	0.3	0.0	0.0
Gibraltar UK	100.0	100.0	100.0	100.0	0.0	0.0
Greece	57.7	25.7	9.4	2.2	0.6	0.1
Grenada	24.5	13.5	3.3	0.0	0.0	0.0
Guadeloupe	89.5	87.5	55.6	10.3	0.0	0.0
Guatemala	16.1	5.8	2.1	0.7	0.2	0.0
Guernsey UK	100.0	100.0	97.7	3.8	0.0	0.0
Guinea	0.4	0.2	0.1	0.0	0.0	0.0
Guinea-Bissau	1.8	0.7	0.2	0.0	0.0	0.0
Guyana	0.4	0.2	0.1	0.0	0.0	0.0
Haiti	5.1	2.1	0.9	0.3	0.0	0.0
Honduras	10.6	4.5	1.8	0.5	0.0	0.0
Hungary	100.0	81.9	29.9	3.4	0.6	0.1
India	34.7	14.9	5.0	0.8	0.1	0.0
Indonesia	6.8	3.3	1.4	0.3	0.0	0.0
Iran	30.2	14.2	6.2	2.0	0.5	0.1
Iraq	25.3	11.5	5.1	2.0	0.5	0.0
Ireland	61.2	22.0	7.0	1.5	0.3	0.0
Isle of Man UK	100.0	65.9	19.1	0.0	0.0	0.0
Israel	90.3	78.0	58.6	35.7	9.4	1.0
Italy	99.4	91.9	58.7	19.1	1.9	0.1
Ivory Coast	2.5	0.9	0.3	0.1	0.0	0.0
Jamaica	93.7	57.4	22.4	5.2	1.0	0.0
Japan	98.5	84.4	53.5	24.0	5.6	1.0
Jersey UK	100.0	100.0	68.4	0.0	0.0	0.0
Jordan	27.2	15.8	9.0	2.1	0.4	0.0
Kazakhstan	4.3	1.9	0.8	0.2	0.0	0.0
Kenya	1.6	0.7	0.3	0.1	0.0	0.0
Kuwait	100.0	88.4	65.0	39.4	13.2	3.5
Kyrgyzstan	12.4	5.3	1.5	0.1	0.0	0.0
Laos	1.7	0.7	0.3	0.0	0.0	0.0
Latvia	34.8	13.0	4.0	1.1	0.3	0.0
Lebanon	100.0	66.0	33.3	6.7	0.3	0.0
Lesotho	3.4	1.2	0.4	0.0	0.0	0.0
Liberia	0.0	0.0	0.0	0.0	0.0	0.0
Libya	8.4	4.1	1.7	0.6	0.1	0.0
Liechtenstein	100.0	100.0	90.6	0.0	0.0	0.0
Lithuania	62.2	21.3	6.9	1.5	0.1	0.0
Luxembourg	100.0	100.0	100.0	61.2	11.6	0.0
Macau P	100.0	100.0	100.0	100.0	100.0	0.0
Macedonia	56.7	19.3	5.6	0.5	0.0	0.0
Madagascar	0.2	0.1	0.0	0.0	0.0	0.0
Malawi	3.4	1.7	0.7	0.2	0.1	0.0
Malaysia	22.2	11.9	5.4	1.6	0.3	0.0
Mali	0.4	0.2	0.1	0.0	0.0	0.0
Malta	100.0	100.0	99.4	73.7	14.4	0.0
Martinique F	100.0	91.9	67.0	16.6	0.0	0.0
Mauritania	0.2	0.1	0.0	0.0	0.0	0.0
Mayotte F	7.9	3.0	0.0	0.0	0.0	0.0
Mexico	30.5	16.1	7.2	2.4	0.6	0.1
Moldova	67.3	26.2	7.1	0.9	0.1	0.0
Monaco	100.0	100.0	100.0	100.0	63.2	0.0
Mongolia	0.3	0.1	0.0	0.0	0.0	0.0
Montenegro	31.3	10.9	2.9	0.1	0.0	0.0
Montserrat UK	56.1	15.8	0.0	0.0	0.0	0.0
Morocco	12.4	4.9	1.7	0.5	0.1	0.0
Mozambique	0.5	0.2	0.1	0.0	0.0	0.0
Myanmar	2.9	1.1	0.3	0.1	0.0	0.0
Namibia	0.7	0.3	0.1	0.0	0.0	0.0
Nepal	3.1	1.2	0.3	0.0	0.0	0.0
Netherlands	100.0	99.1	96.7	56.8	8.3	0.6
Netherlands Antilles	89.3	66.1	43.2	26.8	5.4	0.0
New Caledonia	3.2	1.3	0.6	0.3	0.0	0.0
New Zealand	11.7	5.0	2.1	0.7	0.1	0.0
Nicaragua	8.2	3.3	1.2	0.3	0.0	0.0
Niger	0.2	0.1	0.0	0.0	0.0	0.0
Nigeria	12.4	7.8	5.3	3.0	1.1	0.1
Norfolk Islands AU	2.9	0.0	0.0	0.0	0.0	0.0
North Korea	8.8	3.6	1.1	0.1	0.0	0.0
Norway	62.8	34.6	14.6	4.4	0.9	0.1

Table 3 – *continued*

Country	(1) $\geq 0.11b_n$	(2) $\geq 0.33b_n$	(3) $\geq b_n$	(4) $\geq 3b_n$	(5) $\geq 9b_n$	(6) $\geq 27b_n$
Oman	27.8	12.7	4.8	1.4	0.3	0.0
Pakistan	30.2	19.4	7.9	0.9	0.2	0.0
Panama	11.7	5.4	2.3	0.7	0.1	0.0
Papua New Guinea	2.1	1.0	0.5	0.2	0.0	0.0
Paraguay	4.6	2.0	0.9	0.4	0.1	0.0
Peru	3.0	1.3	0.5	0.2	0.1	0.0
Philippines	12.6	6.2	2.5	0.7	0.2	0.0
Poland	96.8	59.6	23.9	4.3	0.5	0.0
Portugal	85.1	47.8	24.1	6.8	1.1	0.2
Puerto Rico	99.4	98.9	97.2	68.4	11.5	2.2
Qatar	99.3	89.5	55.2	27.5	8.8	2.6
Romania	52.2	20.5	5.9	0.6	0.0	0.0
Russia	24.2	11.1	4.3	1.2	0.2	0.0
Rwanda	2.0	0.8	0.3	0.0	0.0	0.0
Saint Kitts e Nevis	92.3	53.0	22.1	0.0	0.0	0.0
Saint Lucia	60.3	29.7	10.9	0.0	0.0	0.0
San Marino	100.0	100.0	100.0	97.2	0.0	0.0
Saudi Arabia	19.3	9.8	4.5	1.7	0.4	0.1
Senegal	1.3	0.5	0.2	0.1	0.0	0.0
Serbia	72.0	37.3	11.8	1.1	0.1	0.0
Sierra Leone	0.6	0.2	0.1	0.0	0.0	0.0
Singapore	100.0	100.0	100.0	100.0	100.0	33.3
Slovakia	100.0	98.4	64.1	4.8	0.2	0.0
Slovenia	100.0	84.2	29.3	3.1	0.2	0.0
Somalia	0.0	0.0	0.0	0.0	0.0	0.0
South Africa	13.7	6.8	3.0	1.2	0.3	0.0
South Korea	99.7	98.2	79.2	32.0	5.9	1.2
Spain	83.3	50.4	23.0	7.3	1.4	0.2
Sri Lanka	21.6	8.8	2.4	0.0	0.0	0.0
St. Vincent-Grenadines	29.7	13.8	2.4	0.0	0.0	0.0
Sudan	0.8	0.4	0.1	0.0	0.0	0.0
Suriname	1.0	0.4	0.2	0.0	0.0	0.0
Swaziland	11.0	4.1	1.2	0.0	0.0	0.0
Sweden	66.9	49.9	26.6	6.7	1.2	0.1
Switzerland	100.0	97.7	57.4	10.2	0.4	0.0
Syria	50.3	26.6	11.2	3.9	1.0	0.1
Taiwan	90.5	63.1	45.5	27.2	6.4	0.4
Tajikistan	13.1	5.5	1.7	0.0	0.0	0.0
Tanzania	1.5	0.7	0.3	0.1	0.0	0.0
Thailand	33.6	18.1	9.0	2.7	0.5	0.1
Togo	1.3	0.6	0.3	0.0	0.0	0.0
Trinidad and Tobago	89.8	53.7	29.6	10.7	0.1	0.0
Tunisia	28.0	12.6	4.8	1.2	0.1	0.0
Turkey	31.2	12.2	4.1	0.7	0.1	0.0
Turkmenistan	9.2	4.1	1.6	0.4	0.1	0.0
Turks and Caicos Is. UK	15.6	8.7	0.0	0.0	0.0	0.0
Uganda	1.1	0.5	0.2	0.0	0.0	0.0
Ukraine	62.4	31.2	11.1	1.7	0.1	0.0
United Arab Emirates	74.6	50.9	30.2	12.8	3.1	0.7
United Kingdom	84.7	67.9	48.1	20.1	3.5	0.1
United States of America	61.8	42.7	22.5	9.2	2.6	0.6
Uruguay	14.4	5.6	2.3	0.9	0.3	0.0
Uzbekistan	23.4	13.8	6.5	1.0	0.1	0.0
Vanuatu	5.7	4.8	2.7	1.1	0.0	0.0
Venezuela	21.6	10.8	5.1	2.0	0.5	0.0
Vietnam	7.0	2.8	1.0	0.3	0.0	0.0
Virgin islands US	100.0	93.6	77.3	53.2	0.0	0.0
Western Sahara	0.7	0.3	0.1	0.0	0.0	0.0
Yemen	6.1	2.5	0.8	0.2	0.0	0.0
Zaire	0.4	0.1	0.1	0.0	0.0	0.0
Zambia	1.1	0.4	0.2	0.0	0.0	0.0
Zimbabwe	2.6	1.1	0.5	0.1	0.0	0.0
European Union	85.3	64.8	36.7	11.5	1.7	0.1
The World	18.7	10.9	5.3	1.8	0.4	0.1



Figure 9. Artificial night sky brightness at sea level for Oceania. The map has been computed for the photometric astronomical V band, at the zenith, for a clean atmosphere with an aerosol clarity coefficient $K = 1$. The calibration refers to 1996–1997. Country boundaries are approximate.

Vienna United Nations Organization Centre in the summer of 1999 (Cohen & Sullivan 2000).

ACKNOWLEDGMENTS

We are grateful to Roy Garstang of JILA–University of Colorado for his friendly kindness in reading and commenting on this paper, for his helpful suggestions and for interesting discussions. We acknowledge the unknown referee for the stimulus to extend this work with statistical tables. PC acknowledges the Istituto di Scienza e Tecnologia dell’Inquinamento Luminoso (ISTIL), Thiene, Italy, which supported part of this work. The authors gratefully acknowledge the US Air Force for providing the DMSP data used to make the night-time lights of the World.

REFERENCES

- Catanzaro G., Catalano F. A., 2000, in Cinzano P., ed., *Measuring and Modelling Light Pollution*, Mem. Soc. Astron. Ital., 71, 211
- Cinzano P., 1994, *References on Light Pollution and Related Fields version 2*, Internal Report 11, Dep. of Astronomy, Padova, also on-line at <http://www.pd.astro.it/cinzano/refer/index.htm>
- Cinzano P., 2000a, in Cinzano P., ed., *Measuring and Modelling Light Pollution*, Mem. Soc. Astron. Ital., 71, 93
- Cinzano P., 2000b, in Cinzano P., ed., *Measuring and Modelling Light Pollution*, Mem. Soc. Astron. Ital., 71, 113
- Cinzano P., 2000c, in Cinzano P., ed., *Measuring and Modelling Light Pollution*, Mem. Soc. Astron. Ital., 71, 159
- Cinzano P., 2000d, in Cinzano P., ed., *Measuring and Modelling Light Pollution*, Mem. Soc. Astron. Ital., 71, 1
- Cinzano P., Falchi F., 2000, <http://www.pd.astro.it/cinzano/en/sbeam2.html>

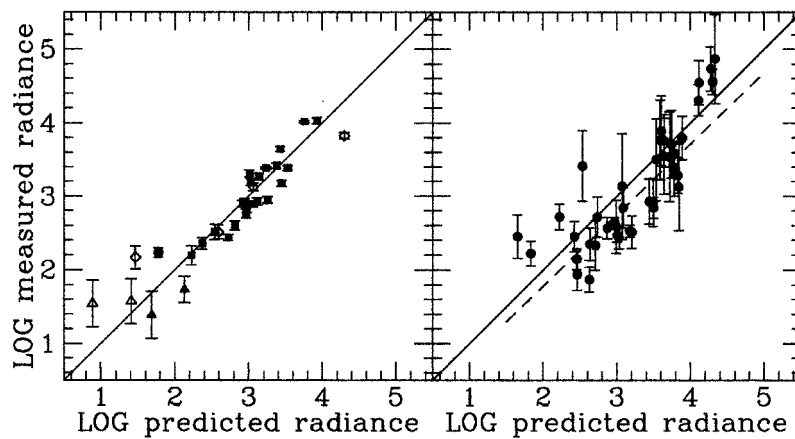


Figure 10. Comparison between map predictions and measurements of artificial night sky brightness. Left panel: map predictions versus artificial sky brightness measurements at the bottom of the atmosphere taken in clean or photometric nights in the V band in Europe (filled squares), North America (open triangles), South America (open rhombi), Africa (filled triangles) and Asia (filled circle). Right panel: map predictions versus photographic measurements taken in Japan in the period 1987–1991 with variable atmospheric aerosol content and averaged for each site. The large error bars show the effects of the changes in the atmospheric aerosol content and in the extinction of the light of the comparison star. The dashed line shows the linear regression. Night sky brightnesses are expressed as photon radiances.

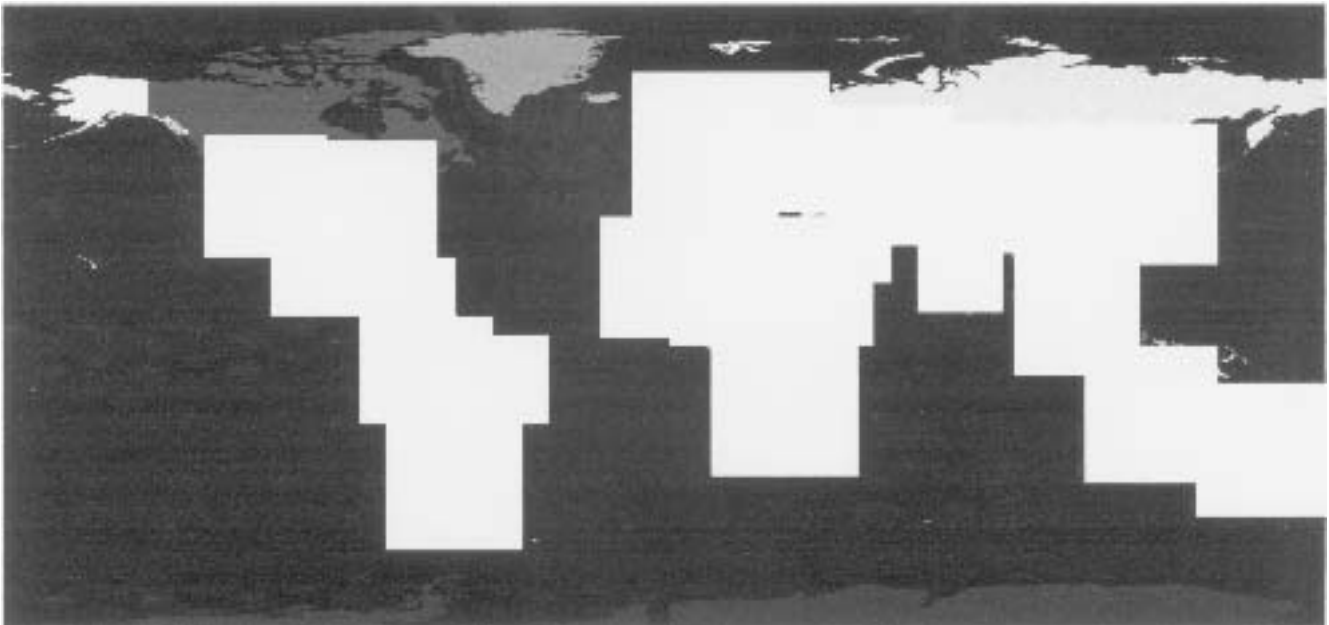


Figure 11. The World areas covered by the Atlas and the statistic (in white).

Cinzano P., Falchi F., Elvidge C. D., Baugh K. E., 2000, *MNRAS*, 318, 641 (Paper I)
 Cinzano P., Falchi F., Elvidge C. D., 2001a, *MNRAS*, 323, 34 (Paper II)
 Cinzano P., Falchi F., Elvidge C. D., 2001b, *Earth, Moon and Planets*, 85, 517
 Cohen J., Sullivan W. T., eds, 2001, *Proc. UN–IAU Symp. 196, Preserving the Astronomical Sky*. Astron. Soc. Pac., San Francisco
 Crawford D. L., ed., 1991, *ASP Conf. Ser. Vol. 17, IAU Coll. 112, Light Pollution, Radio Interference and Space Debris*. Astron. Soc. Pac., San Francisco
 Della Prugna F., 1999, *A&AS*, 140, 345
 Dobson J. E., Bright E. A., Coleman P. R., Durfee R. C., Worley B. A., 2000, *Photogrammetric Engineering and Remote Sensing*, 66, 849
 Elvidge C. D., Baugh K. E., Kihn E. A., Kroehl H. W., Davis E. R., 1997a, *Photogram. Eng. Remote Sens.*, 63, 727
 Elvidge C. D., Baugh K. E., Kihn E. A., Kroehl H. W., Davis E. R., Davis C., 1997b, *Int. J. Remote Sensing*, 18, 1373

Elvidge C. D., Baugh K. E., Hobson V. H., Kihn E. A., Kroehl H. W., Davis E. R., Cocero D., 1997c, *Global Change Biology*, 3, 387
 Elvidge C. D., Baugh K. E., Dietz J. B., Bland T., Sutton P. C., Kroehl H. W., 1999, *Remote Sens. Environ.*, 68, 77
 Elvidge C. D., Imhoff M. L., Baugh K. E., Hobson V. R., Nelson I., Dietz J. B., 2001, *J. Photogrammetry and Remote Sensing*, submitted
 Falchi F., 1998, *Tesi di Laurea*, Univ. Milan
 Falchi F., Cinzano P., 2000, in Cinzano P., ed., *Measuring and Modelling Light Pollution*, *Mem. Soc. Astron. Ital.*, 71, 139
 Favero G., Federici A., Blanco A. R., Stagni R., 2000, in Cinzano P., ed., *Measuring and Modelling Light Pollution*, *Mem. Soc. Astron. Ital.*, 71, 223
 Garstang R. H., 1984, *Observatory*, 104, 196
 Garstang R. H., 1986, *PASP*, 98, 364
 Garstang R. H., 1989a, *PASP*, 101, 306
 Garstang R. H., 1989b, *ARA&A*, 27, 19
 Garstang R. H., 1991, *PASP*, 103, 1109

- Garstang R. H., 2000, in Cinzano P., ed., *Measuring and Modelling Light Pollution*, Mem. Soc. Astron. Ital., 71, 83
- Isobe S., Hamamura S., 1998, in Isobe S., Hirayama T., eds, ASP Conf. Ser. Vol. 139, Proc. IAU JD5, *Preserving the Astronomical Windows*. Astron. Soc. Pac., San Francisco, p. 191
- Isobe S., Hirayama T., eds, 1998, ASP Conf. Ser. Vol. 139, Proc. IAU JD5, *Preserving the Astronomical Windows*. Astron. Soc. Pac., San Francisco
- Kosai H., Isobe S., Nakayama Y., 1992, Proc. IDA Annual Meeting 65
- Kovalevsky J., ed., 1992, *The Protection of Astronomical and Geophysical Sites*, NATO Pilot Study no. 189. Editions Frontieres, Paris
- Krisciunas K., Schaefer B. E., 1991, PASP, 103, 1033
- Lieske R. W., 1981, Proc. Int. Telemetry Conf., 17, 1013
- McNally D., ed., 1994, Proc. IAU-ICSU-UNESCO meeting *Adverse environmental impacts on astronomy, The Vanishing Universe*. Cambridge Univ. Press, Cambridge
- Massey P., Foltz C. B., 2000, PASP, 112, 566
- Nawar S., Morcos A. B., Metwally Z., Osman A. I. I., 1998a, in Isobe S., Hirayama T., eds, ASP Conf. Ser. Vol. 139, *Preserving the Astronomical Windows*. Astron. Soc. Pac., San Francisco, p. 151
- Nawar S., Morcos A. B., Mikhail J. S., 1998b, Ap&SS, 262, 485
- Piersimoni A., Di Paolantonio A., Brocato E., 2000, in Cinzano P., ed., *Measuring and Modelling Light Pollution*, Mem. Soc. Astron. Ital., 71, 221
- Poretti E., Scardia M., 2000, in Cinzano P., ed., *Measuring and Modelling Light Pollution*, Mem. Soc. Astron. Ital., 71, 203
- Schaefer B. E., 1993, *Vistas Astron.*, 36, 311
- Smith F. G., 1979, IAU Trans., XVIII, 218
- Sullivan W. T., 1989, Int. J. Remote Sensing, 10, 1
- Sullivan W. T., 1991, in Crawford D. L., ed., ASP Conf. Ser. Vol. 17, IAU Coll. 112, *Light Pollution, Radio Interference and Space Debris*. Astron. Soc. Pac., San Francisco, p. 11
- Walker M., 1987, NOAO Newsl., 10, 16
- Zitelli V., 2000, in Cinzano P., ed., *Measuring and Modelling Light Pollution*, Mem. Soc. Astron. Ital., 71, 193

This paper has been typeset from a T_EX/L^AT_EX file prepared by the author.